The impact of formulation and 3D-printing on the catalytic properties of ZSM-5 zeolite

The impact of formulation and 3D-printing on the catalytic properties of ZSM-5 zeolite

J. Lefevere, S. Mullens, V. Meynen

PII: S1385-8947(18)30847-7
DOI: https://doi.org/10.1016/j.cej.2018.05.058
Reference: CEJ 19074

To appear in: *Chemical Engineering Journal*

Received Date: 3 November 2017
Revised Date: 13 April 2018
Accepted Date: 7 May 2018

Please cite this article as: J. Lefevere, S. Mullens, V. Meynen, The impact of formulation and 3D-printing on the catalytic properties of ZSM-5 zeolite, *Chemical Engineering Journal* (2018), doi: https://doi.org/10.1016/j.cej.2018.05.058

The impact of formulation and 3D-printing on the catalytic properties of ZSM-5 zeolite

Lefevere J.[1,2], Mullens S.[1], Meynen V.[1,2]

[1] *Flemish Institute for Technological Research (VITO), Boeretang 200, 2400 Mol, Belgium.*

[2] *University Antwerp, Laboratory of Adsorption and Catalysis, Universiteitsplein 1, 2610 Wilrijk, Belgium.*

Abstract

Structured catalysts can help to overcome the drawbacks of conventional packed bed catalysts and help to make more efficient use of the catalytic material in the reactor. One of the major disadvantages of coated structured catalysts is the limited catalyst loading per reactor volume. In this paper, a robocasting 3D-printing technique was used to manufacture self-supporting macroporous ZSM-5 structures and so overcome the issue of low loading. Moreover, 3D-printing offers the possibility to optimize the architecture of the structured catalyst. In this work, methanol-to-olefins (MTO) was used as a test reaction to investigate the impact of 3D-printing on catalytic properties without changing the basic catalytic start material. Firstly, the influence of different binders and binder combinations in the self-supporting structured catalyst is discussed. Secondly, the architecture of the catalyst was varied by changing the diameter of the fibers of the structure, the porosity of the structure and the shape of the channels in the direction of the flow. The results show a significant impact of both the binders and the architecture on the catalytic properties of ZSM-5 for the methanol-to-olefins reaction.

Keywords: 3D-printing; binders; ZSM-5; methanol-to-olefins; structured catalyst

Introduction

In industry, catalysts are commonly used in the form of packed beds of pellets, which can however suffer from mass and heat transfer limitations. Reducing the size of the pellets can improve the mass and heat transfer, however, this increases the pressure drop over the catalyst bed. Structured supports, such as foams or honeycombs, offer significantly lower pressure drops [1–3]. These types of supports coated with a thin layer of active material can exhibit good mass and heat transfer properties. Mostly, wash coating or hydrothermal coating methods are used to apply the active layer on the support [4,5]. These structures exhibit the good mechanical properties of the support

and have a low consumption of active material. Nevertheless, they struggle with issues such as the anchoring of the coating material particles and the uniformity of the coating throughout the structures [6,7]. Another major drawback of these types of coated catalytic structures is the limited amount of catalyst per reactor volume. Repeated coating steps can help to increase the loading, however the loading remains much lower than that of a packed bed. An interesting alternative is a bulk catalytic (self-supporting) structured catalyst. In this way, no volume in the reactor is lost on inert support material, at the condition that all active material is accessible through the pores of the structures. Furthermore, direct synthesis of inherent catalytic structures requires less process steps than manufacturing of a support followed by one or multiple coatings.

One way of manufacturing a self-supporting zeolite honeycomb is direct extrusion of a zeolite containing paste. In literature, both ZSM-5 and zeolite A-5 have been successfully manufactured in a monolith shape [8–11]. The use of both organic and inorganic binders in the composition of the extrusion paste was necessary to obtain good rheology of the paste and sufficient drying and firing properties. Compared to the cordierite structures, the mechanical properties of zeolite monoliths are worse, so permanent binders are needed to increase the mechanical strength. However, in previous work it has been shown that just like with pellets, these binders will have an impact on the physico-chemical and thus catalytic properties of the final catalyst [12–14]. The use of 3D-printing of a catalyst allows for a high degree of freedom in both composition and design of the final catalyst material.

Honeycomb monoliths are often used as structured catalytic supports in applications with high flow rates. For catalysis, the fact that honeycomb type of catalysts have no radial mass and heat transfer may be disadvantageous for a lot of applications. In highly exothermic reactions such as methanol-to-olefins (MTO), temperature increase can lead to permanent deactivation of the catalyst [15,16]. As discussed in previous work, a possible solution can be found in robocasting, a 3D-printining technique, in order to rapidly prototype different compositions and architectures of a zeolite structured catalyst system [17]. 3D-printing is a rapid growing field with many papers concerning the use of these type of materials in catalysis [18–21] or sorption [22–24]. One major benefit of direct printing of a porous material is the flexibility of design of the final structure since the porosity, internal architecture and wall thickness can be altered in function of the application [25]. It has already been shown that the stacking geometry of the layers of a 3D-printed structure will have an impact on the selectivity and activity of the catalytic coating on the structured support in MTO [17]. Moreover, modeling studies suggested that the wall thickness and the porosity of the

structure will have an impact on the selectivity in the methanol-to-propylene (MTP) reaction [26,27]. This effect is assigned to the difference in mass transfer properties. However, the advantages of architectural design as described in these modeling studies have not yet been shown in experimental studies. Moreover, the combination of binders to achieve both mechanical and physico-chemical desired properties next to architectural design has not yet been studied for the 3D-printing process.

In this work, the impact of the use of different binders and geometries in 3D-printed ZSM-5 structures on its catalytic performance in the methanol-to-olefins reaction are discussed. In order to evaluate the impact of shaping, a robocasting 3D-printing technique was chosen to achieve comparable material characteristics as to extrudates. The impact of different binders and combinations of these binders on the catalytic properties are investigated. In a second part, the influence of the architecture on the selectivity and stability of the catalyst are shown for the best catalyst-binders combination composition. The porosity, fiber thickness and stacking of the layers have been varied to reveal their impact.

Materials and methods

Preparation of the catalysts

ZSM-5 zeolite (Si/Al ratio = 25) was provided by Süd-chemie and used as received. The inorganic binders used were: bentonite (VWR), colloidal silica (Ludox HS-40, Sigma Aldrich) and aluminophosphate solution (Litopix P-1, Zschimmer und Schwartz). The fraction of bentonite powder smaller than 45 µm was used in the catalyst formulation. The procedure for the 3D-printing process was described in more detail in the previous work [28]. All organic binder (methylcellulose) was removed during calcination for 3 hours at 550 °C before use.

The structures were built up by extrusion of the zeolite/binder paste through a thin nozzle that follows a computer controlled movement in x, y and z direction. The in-house build robocasting device uses a stepper driven plunger to feed the paste into the nozzle. A feed rate of 1500; 600 and 200 µl/min was applied respectively for the 1500, 900 and 400 µm nozzles. All the 3D –printing was performed at room temperature, no additional heating was applied to the paste during 3D-printing. Using this procedure, structures with different binder composition were synthesized, the zeolite/inorganic binder ratio was 65/35 weight percent for all samples. A detailed description of the manufacturing process and impact on mechanical and physico-chemical properties can be

found in previous work [29]. In a first series, single binder structures with bentonite, silica and aluminophosphate binders in combination with ZSM-5 as catalyst were produced (single-binder structures). During the printing process, the nozzle diameter was kept at 0.9 mm and the porosity of the structure was programmed to be 68 %. Secondly, binary binder structures were manufactured and tested using 50/50 ratio of two different binders while maintaining 65/35 weight percent ZSM-5 and total amount of binders. In case of silica/aluminophosphate binary-binder systems, structures with different architectures were manufactured as well. Firstly, the thickness of the fibers was varied ranging from 0.4 mm up to 1.5 mm by varying the nozzle diameter. Secondly, the open frontal area of the structure was changed at a constant nozzle size of 0.9 mm by altering the distance between the fibers. Open frontal areas of 32, 38 and 42 % and a porosity of respectively 55, 68 and 75 % were used. As the mass of the catalyst was kept constant during the testing, the length of the bed increased with higher porosity of the catalyst. Finally, structures with alternative stacking of the layers were used. In the standard structure (1-1) all layers were stacked on top of each other resulting in straight channels, whereas for the altered stacking (1-3) the layers were shifted resulting in zigzag channels in the direction of the flow (Figure 1). In order to evaluate the difference between the structured catalysts and a packed bed, also pellets with the same zeolite/binder composition were produced by extrusion. These extrudates had a diameter of 2 mm and a length of 15 mm. The same loading of catalyst in the reactor was applied for testing of all samples.

Characterization

The acidity of the catalyst materials was analyzed using 2-cycle NH_3 adsorption (TCA) coupled to a temperature programmed desorption (TPD) [30]. Prior to the analysis, the catalyst materials were degassed at 200 °C under high-vacuum conditions for 16 hours. The degassing, TCA and TPD measurements are all carried out on a Quantachrome Autosorb-iQ-C equipped with a thermal conductivity detector (TCD). Before starting the acidity study, the dry weight of the samples was measured followed by a second degassing step at 200 °C under a flow of helium in order to avoid any adsorbed molecules on the samples. After a leak test to certify the degassing of the set-up, the temperature was lowered to 100 °C, at which the TCA is measured. The first adsorption cycle of ammonia was recorded, after which the samples were degassed for 45 min at 100°C under high-vacuum. Subsequently, the second ammonia adsorption phase followed at 100 °C. In the first cycle the ammonia adsorbs both chemically as physically on the sample. Whereas in the second cycle only the physically adsorbed ammonia molecules are recorded because the intermediate degassing

step only removes the weakly bound (physically adsorbed) ammonia from the sample. From the difference between the two isotherms the total number of chemisorbed ammonia molecules can be calculated, which corresponds to number of acid sites on the catalyst material. The acid site concentration can be calculated either by weight or by specific surface area (using nitrogen sorption). In order to remove the physisorbed ammonia from the sample before the TPD, another degassing step was performed at 100 °C under a flow of helium until the signal of the TCD detector decreased to the level of the baseline. In the temperature programmed desorption the strength of the acid sites is analyzed by increasing the temperature from 100 to 750 °C at a rate of 10 °C min^{-1} under a flow of helium and recording the desorption of ammonia with the TCD. The weak and strong acid sites were respectively assigned to the areas between 100 - 200 °C and 200 - 550 °C. The peaks above 550 °C were not taken into account as there might be a contribution of water by dehydroxylation at temperatures higher than the calcination temperature.

The specific surface area and pore volume under 50 nm was measured for all self-supporting catalyst materials and ZSM-5 by nitrogen sorption at 196 °C using a Quantachrome Autosorb-1. Before the surface analysis, the materials were degassed for 16 hours at 200 °C in order to remove all adsorbed water from the surface. Using the BET method, the total surface area was calculated, while the t-plot was used to differentiate between micropore and external surface. At P/P_0 the total pore volume lower than 50 nm was calculated. Larger pores up to 10 µm were analyzed using Hg-porosimetry (Pascal Mercury Porosimeters, Thermo Scientific).

Catalytic tests

The catalytic performance of the self-supporting catalysts and the zeolite was evaluated in a fixed bed alumina reactor with an inner diameter of 22 mm. In a first phase the activity of the catalyst materials was tested using 1 g of sample at temperatures form 300 up to 450 °C. Next, the stability of the samples was assessed using 3.34 g of catalyst at a temperature of 450 °C and atmospheric pressure. The manufactured samples were placed in the middle of the reactor zone, fixed with a layer of quartz wool. The reactor can be considered as quasi-adiabatic as the heat transfer coefficients of the quartz wool and alumina of the reactor are very low. The oven around the reactor keeps the temperature isothermal at the reactor entrance. If heat is produced due to the exothermic nature of the reaction a temperature increase in the catalytic bed is possible. However, no extra cooling of the reactor was applied. The structures were composed of a weight fraction of

65 percent of zeolite and 35 percent of binder(s). Table 1 gives an overview of the different catalysts tested.

Methanol (Merck, ≥ 99.9 %) was fed at a rate of 0.1 ml/min using a HPLC pump and diluted with nitrogen gas at a rate of 300 ml/min. In order to achieve a homogenous flow of the reaction mixture, the methanol was evaporated and mixed with nitrogen in an isothermal reservoir at 200 °C and fed to reactor through heated lines. The reaction enthalpy for MTO is -4.6 kcal/mol (-0.54 kJ/g_{MeOH}) [14]. A gas chromatograph with flame ionization detector (450-GC, Bruker) was used to analyze the conversion and product distribution. In the activity testing, the conversion was monitored for 1 h at each temperature. In the stability test the samples were analyzed until deactivation of the samples occurred. In the data analysis, all C_5+ species are combined in one group as this is not the main focus of this research and dimethyl ether (DME) was regarded as a reactant. The selectivity was determined for each sample at 90 % conversion during the stability experiments as the conversions showed large differences in the activity experiments.

Table 1: Overview of catalytic structures investigated.

Sample code	Zeolite (wt%)	Binder(s) (wt%)	Fiber thickness (µm)	Stacking of layers
ZSM-5	ZSM-5 (100)	-	2000	Pellets
Bentonite	ZSM-5 (65)	bentonite (35)	900	1-1
SiO_2	ZSM-5 (65)	silica (35)	900	1-1
$AlPO_4$	ZSM-5 (65)	aluminophosphate (35)	900	1-1
Bent/SiO_2	ZSM-5 (65)	bentonite (17.5) silica (17.5)	900	1-1
Bent/$AlPO_4$	ZSM-5 (65)	bentonite (17.5) aluminophosphate (17.5)	900	1-1
$AlPO_4/SiO_2$	ZSM-5 (65)	silica (17.5) aluminophosphate (17.5)	900	1-1
$AlPO_4/SiO_2$_1-3	ZSM-5 (65)	silica (17.5) aluminophosphate (17.5)	900	1-3
$AlPO_4/SiO_2$_pellets	ZSM-5 (65)	silica (17.5) aluminophosphate (17.5)	2000	Pellets
$AlPO_4/SiO_2$_400	ZSM-5 (65)	silica (17.5) aluminophosphate (17.5)	400	1-1
$AlPO_4/SiO_2$_1500	ZSM-5 (65)	silica (17.5) aluminophosphate (17.5)	1500	1-1
$AlPO_4/SiO_2$_55 % porosity	ZSM-5 (65)	silica (17.5) aluminophosphate (17.5)	900	1-1
$AlPO_4/SiO_2$_75 % porosity	ZSM-5 (65)	silica (17.5) aluminophosphate (17.5)	900	1-1

Results and discussions

Effect of binder on catalysis

Single binder systems

The conversion of methanol with single binder catalysts at different temperatures (Figure 2) shows a lower activity of the aluminophosphate binder catalyst. At 450 °C both the silica and bentonite bound samples show similar conversion around 90 % whereas the aluminophosphate sample only shows just over 50 % conversion. The stability testing with a larger amount of catalyst (Figure 3), shows a faster deactivation for the sample with aluminophosphate as binder compared with bentonite or silica as binder. Clearly, the aluminophosphate binder has a major impact on the active sites of the zeolite. It was already suggested in literature that the phosphate component from the binder can diffuse into the pores and interact with the active sites of the ZSM-5 zeolite [31,32] as also visible from the physico-chemical data (Table 2 – Figure SI1, Supplementary data). All 3D-printed samples show lower stability compared to the pure ZSM-5 zeolite, mainly because they have only 65 weight percent of the active component.

Although the mechanism of this aluminophosphate binding is still under discussion, interesting observations can be made. The results of nitrogen sorption and the 2-cycle TPD measurement suggest that the interaction between the phosphate ions and the acid sites leads to a significant decrease in surface area and pore volume (below 50 nm) of the zeolite (Table 2), but an increase of acid sites per surface area on the remaining surface. However, the acid strength of these sites is clearly much less compared to the pure zeolite (Figure SI 1). The loss of micropore area and low acid site strength could explain the low conversion.

Both the silica/ZSM-5 and bentonite/ZSM-5 catalysts show a loss in acid density on the surface(~ 46 % and 37 % respectively) compared to the pure ZSM-5, possibly due to a low content of sodium ions in the binders. The decrease caused by the Ludox HS-40 silica binder is higher compared to the bentonite binder, as it has the highest sodium content. Furthermore, the diffusivity of methanol to the active site may also play a role as the meso/micropore volume is higher in the sample with silica as binder. The close proximity of binder and zeolite particles clearly have an impact on catalytic properties, as was confirmed by literature [33,34].

Table 2: Results of N_2-sortpion, Hg-porosimetry and 2-cycle NH_3-TPD on pure zeolite and different single binder structures (65/35 weight ratio zeolite/binder) after calcination.

Structure	BET surface area (m^2/g)	Micropore surface area (m^2/g)	Pore volume < 50 nm (cm^3/g)	Macropore volume (cm^3/g)	Number of acid sites ($1/Å^2$)	Number of acid sites (µmol/g)
Pure H-ZSM-5	428	379	0.159	-	1.17	834.0
Bentonite	292	250	0.185	0.432	0.74	361.0
Silica	305	234	0.266	0.275	0.64	322.5
$AlPO_4$	124	118	0.061	0.407	2.62	710.1

The measurements show that the binder type also has a significant impact on the selectivity to light olefins in the MTO reaction for the catalysts prepared with a single binder (Table 3). The $AlPO_4$-sample exhibits higher selectivity towards the desired products, while for the bentonite and silica binder catalysts, the production of undesired methane and alkanes is much higher. The lower number of strong acid sites and lower micro/mesoporosity of the catalyst with the aluminophosphate binder results in superior selectivity towards propylene and a higher selectivity to heavier alkenes being mainly pentenes. The silica and bentonite binder systems, with higher density of strong acid sites, show high methane and alkane formation. The pure ZSM-5 pellets however, show even higher production of undesired side products (C_2-C_4 alkanes). These results suggest that uncontrolled side reactions occur when high amounts of strong acidity and longer residence time in the microporous zone is present. These observations are in agreement with earlier work where aluminophosphate was shown to lower the strong acidity, resulting in higher selectivity towards propylene [14,31,32]. Another work of Ahmadpour et al. showed that for longer contact time in the micropores, the selectivity towards propylene decreases. It should be noted that ratio between the macropore volume and surface area or micro/mesopore volume is much higher for the sample with $AlPO_4$ binder, so the contact time may be lower. Lee et al. [31] reported that there is a decrease in pore volume and specific surface area of the zeolite with increasing phosphorous concentration in the $AlPO_4$ binder. As the Al/P ratio in the $AlPO_4$ binder used in this work is high, this strong decrease in surface area and pore volume (<50nm) was indeed observed, next to the lowered strong acidity. From table 3 it is clear that this has a significant effect on the selectivity in the MTO reaction. The loss in both strong acidity and surface area of the micropores results in fewer methylbenzenes inside the reaction zone of the zeolite. As propylene and higher alkenes are preferably formed through methylation and cracking cycles of alkenes, while ethylene is mostly formed from the (poly)methylbenzene methylation and dealkylation cycle, lower concentration of methylbenzenes will suppress ethylene formation and secondary dealkylation reactions [35]. In this way, the contribution of the C_3^+ alkene mechanism will increase and lead to higher propylene and heavy alkene concentrations. On the other hand, pure ZSM-5 pellets showed

the reverse effect, the higher acidity and surface area led to a higher selectivity in alkanes and lower propylene/ethylene ratio. The high concentration of methylbenzenes increases the ethylene and secondary dealkylation reactions, resulting in a high undesired selectivity towards alkanes.

Table 3: Selectivity (%) of single binder catalysts at 90 % methanol conversion (65 wt% ZSM-5/35 wt% binder, 450 °C, 3.34 g catalyst).

Sample	CH_4	C_2H_4	C_3H_6	C_4H_8	C_2-C_4 alkanes	C_5^+
ZSM-5 pellets	6.4	13.6	12.2	23.8	27.5	16.5
Bentonite	12.4	17.5	25.0	14.6	6.9	23.6
Silica	9.8	20.7	14.1	17.7	10.3	27.4
$AlPO_4$	1.3	12.4	42.2	11.4	1.9	30.8

Binary binder systems

At temperatures from 300 up to 350 °C the conversion of the sample with double binder bentonite/silica was higher compared to the other binary binder systems. However, at higher temperatures all samples showed nearly full conversion, also when aluminophosphate was present (Figure 4). Conversion of methanol as a function of TOS for the binary binder systems showed an increase in stability in comparison to the single binder systems (Figure 5). Especially the catalyst with aluminophosphate binder in combination with a silica binder exhibits a very good stability, even superior to the pellets of pure ZSM-5 pellets.

The 2-cycle NH_3-TPD measurement and N_2-sorption (Table 4 and Figure SI2 - Supplementary data) clearly shows that the aluminophosphate concentration has a major impact on the acidity of the final catalyst. The decrease in strong acidity of the sample is less in the binary aluminophosphate samples compared with the single aluminophosphate sample. Moreover, there is a smaller decrease in surface area and smaller increase in acid sites per surface area compared to the single binder system. The synergetic effect between the two binders clearly indicates that a binder-binder interaction occurs. The low pH of the aluminophosphate binder solution could affect the stability and surface charge of the colloidal silica and bentonite may partially dissolve at such low pH. Nevertheless, the nature of this interaction and their interaction with the zeolite is not fully understood. Furthermore, for the silica/bentonite sample, the stability is significantly higher than for the single silica and single bentonite system, again indicating a synergic effect. It seems that the binder-binder interaction has an additional effect next to the binder-zeolite interaction.

Table 4: Results of N_2-sortpion, Hg-porosimetry and 2-cycle NH_3-TPD on pure zeolite and different binary binder structures (65/35 weight ratio zeolite/binder) after calcination.

Structure	BET surface area (m^2/g)	Micropore surface area (m^2/g)	Pore volume < 50 nm (cm^3/g)	Macropore volume (cm^3/g)	Number of acid sites ($1/Å^2$)	Number of acid sites (µmol/g)
H-ZSM-5	428	379	0.159	-	1.17	834.0
Bentonite/$AlPO_4$	219	140	0.111	0.553	1.47	533.0
Bentonite/ Silica	301	242	0.282	0.425	0.8	401.3
Silica/ $AlPO_4$	177	126	0.051	0.276	1.77	520.8

The selectivity of methanol to light olefins of the silica/aluminophosphate catalyst is very similar to that of the single binder aluminophosphate catalyst (Table 5). However, the stability of this binary binder catalyst has shown to be significantly higher than that of the pure aluminophosphate binder sample. The catalyst exhibits high selectivity towards propylene and shows a high propylene/ethylene ratio. The heavy alkenes make up a large part of the products, whereas the methane and alkane production is limited, due to major influence of the methylation and cracking cycles of alkenes on the selectivity and limited use of the (poly)methylbenzene methylation and dealkylation cycle. These results suggest that the macropore volume is less crucial in controlling the selectivity and the lower ratio between pore area/volume resulting in lower residence time might be more important. The selectivity of the bentonite/aluminophosphate catalyst towards light olefins is in the middle of the single binder aluminophosphate and the bentonite catalysts. The characterization also confirms that it shows porosity and acidity (Supplementary data) in between that of the single binder samples. Finally, the bentonite/silica containing sample exhibits similar behavior as the single silica and bentonite binder catalysts, with its highly undesired methane and alkane production due to the use of the (poly)methylbenzene route as major pathway.

Table 5: Selectivity (%) of single binder catalysts at 90 % methanol conversion 65 wt% ZSM-5/35 wt% binder, 450 °C, 3.34 g catalyst).

Sample	CH_4	C_2H_4	C_3H_6	C_4H_8	C_2-C_4 alkanes	C_5^+
ZSM-5 pellets	6.4	13.6	12.2	23.8	27.5	16.5
Bent/Silica	8.9	17.7	22.7	16.6	8.0	26.1
Bent/$AlPO_4$	4.4	19.1	33.0	13.9	7.6	22.0
Silica/$AlPO_4$	1.8	9.3	42.3	14.5	3.0	29.1

Influence of architecture

Effect of fiber diameter

As the catalyst with the silica/aluminophosphate binder showed the highest yield of light olefins and a superior TOS stability, different architectures of this catalyst were 3D-printed in order to further improve the catalyst. In a first step the impact of the fiber diameter was evaluated. The results of catalytic testing of structures with fiber diameters of 400, 900 and 1500 µm are shown in

Figure 6 and 7 and Table 6. The results suggest that there is an increase in activity and stability with decreasing fiber diameter. This can be a result of the shorter diffusion path inside of the fibers of the structures. As the diameter of the struts increases, the reactants possibly diffuse too slowly to reach the middle of the catalyst and the center of the fibers of the structure remain unused or less used. On the other hand, the diameter of the fibers influences the residence time in the fiber, which can also influence the coking rate. So clearly the diffusivity and diffusion path inside the catalyst structure will have an impact on the activity and stability of the catalyst as the zeolite/binder combination and thus the acidity is similar. Interestingly, the selectivity towards propylene and light olefins does not change significantly with decreasing fiber diameter (Table 6). This proves that there is no difference in reaction mechanism in the samples with different fiber diameter further supporting the hypothesis that the difference in deactivation appears more probably due to a difference in available surface area.

Table 6: Selectivity (%) of structures with different fiber diameter at 90 % methanol conversion (65 wt% ZSM-5/35 wt% binder, 450 °C).

Sample	CH_4	C_2H_4	C_3H_6	C_4H_8	C_2-C_4 alkanes	C_5^+
1.5 mm	2.1	12.2	41.2	13.2	3.2	28.1
0.9 mm	1.8	9.3	42.3	14.5	3.0	29.1
0.4 mm	2.1	12.1	40.9	13.9	3.9	27.1

Effect of structural porosity

The conversion at different temperatures shows an effect of porosity and open frontal area on the activity of the catalyst (Figure 8). The denser structure, so with less open frontal area, shows higher conversion at lower temperatures compared with catalysts with a more open structure. On the other hand, the results of time-on-stream experiments for the MTO reaction with catalytic structures that differ in macroporosity show that at higher porosity (75 %), the stability increases significantly (~ factor of 2) compared to the standard catalyst with 68 % porosity (Figure 9). The denser sample with 55 % porosity in the structure exhibits a reduced stability. As the difference in porosity is solely a result of difference in open frontal area, the gas velocity through the structure is higher or lower according to the higher and lower porosity of the structure. In this way, also the mass and heat transfer properties are affected. The results show that this increased mass and heat transfer in the structure with low porosity benefits the activity of the catalyst but lowers its stability.

The lower bulk mass and heat transfer in case of large pores in direction of the flow can also result in a lower concentration of methanol on the catalyst surface at the entrance of the reactor. Hence, less heat will be released locally and thus the generation of heat from the exothermic MTO reaction could be spread out over a longer length of the catalyst bed for the same amount of catalysts. The bed is thus more dispersed and in this way, coking can be reduced. This is also supported by observations taken during the initial start-up of the reaction. The initial activity in the bed with higher porosity is lower, taking more time to reach full conversion compared to the samples with lower porosity (45 min with 78 % porosity versus 30 min with 55 and 68 %). This agrees with the conversion experiments showing lower activity for structures with high porosity. Furthermore, 100 % conversion was never reached in the catalyst bed with highest porosity (75%). Moreover, it cannot be excluded that the reactor is not fully adiabatic and some heat transfer via the surface of the reactor occurs, when this would be the case, the longer bed can exchange more heat with the outside. Thus, the temperature rise in the catalyst bed due to the exothermic nature of the reaction could be lower compared to the structures with lower porosity.

There is no clear difference in propylene selectivity between the samples with different porosity (Table 7). If ethylene yield and heavier components are compared however, there seems to be a slight difference. This may be due to the higher temperature in the catalyst bed as more methanol is converted in a smaller volume and so the cracking reaction is increased. These observations were confirmed by literature [17,18]. The cracking rate of the heavier alkenes increases, resulting in the higher ethylene yield and lower yield of C_5-C_7 alkenes. In addition, the increased pressure drop in the structure with lowest porosity could have an impact on the selectivity. It was already shown by Hajimirzaee et al. that increased pressure in MTO over ZSM-5 favors ethylene and alkane production [19]. Moreover, in that work a lower stability was observed at higher pressure. It was suggested that the higher pressure increased the influence of the hydrogen transfer reaction. This relates to the observations found in this work. Although a difference in selectivity is observed for the sample with 55% porosity, no differences can be observed in the samples of 68 and 78% porosity. This indicates that temperature differences will be small or other aspects also play a determining role. It should also be noted that although no large differences occur in selectivity, deactivation appears much faster in the material with 55% and 68% porosity than the highly porous 78% structure.

Table 7: Selectivity (%) of structures with different porosity at 90 % methanol conversion (65 wt% ZSM-5/35 wt% binder, 450 °C, 3.34g catalyst).

Sample	CH_4	C_2H_4	C_3H_6	C_4H_8	C_2-C_4 alkanes	C_5^+
75%	1.4	9.4	43.1	14.4	2.1	29.5
68%	1.8	9.3	42.3	14.5	3.0	29.1
55%	1.5	14.1	41.7	15	4.4	23.3

Effect of fiber stacking

From the conversion measurements at different temperatures it is clear that a randomly packed bed of catalyst pellets shows a significant lower conversion compared to a structured packing (Figure 10). Moreover, the structured packing with a 1-3 stacking, thus zigzag channels in the direction of the flow, has a higher activity than the structure with straight channels. The high turbulence created by these zigzag channels has a major impact on the mass and heat transfer properties of the catalyst. The low conversion with the pellets of catalyst, despite turbulence in the flow, might be a result of the larger diameter of these pellets (2 mm) and/or the non-homogenous flow distribution in the catalyst bed.

On the other hand, the packed bed of pellets as well as the catalytic structure of 1-3 stacking with 68 % porosity showed significant improvement in stability compared to the standard structure with straight channels (Figure 11). Although the initial conversion of the 1-1 structure with straight channels is higher compared to the pellets, the deactivation is faster. It should be noted that these pellets have the same zeolite-binder composition as the 3D-printed structures.

There is a slight difference in selectivity towards propylene in the structure with straight channels compared to the structure with zigzag channels and the pellets (Table 8). It is suggested that the turbulence of the flow, created when using a packed bed or structure with zigzag channels is more efficiently removing the heat of the reaction from the structure resulting in slower deactivation by coking and less side reactions.

Table 8: Selectivity (%) of structures with different stacking of layers at 90 % methanol conversion (65 wt% ZSM-5/35 wt% binder, 450 °C, 3.34g catalyst).

Sample	CH_4	C_2H_4	C_3H_6	C_4H_8	C_2-C_4 alkanes	C_5^+
1-1 (Straight channels)	1.8	9.3	42.3	14.5	3.0	29.1
Pellets	0.7	5.8	47.1	13.9	0.9	31.6
1-3 (Zigzag channels)	1.2	7.4	47.2	14.3	1.9	28.0

Conclusions

The clear impact of different binders used in the 3D-printing of ZSM-5 structured catalysts on the activity, stability and selectivity in conversion of methanol to olefins was demonstrated in this work. It seems that when using an aluminophosphate binder, the acidity and specific surface area decreased, and the selectivity to light olefins was improved. However, when the aluminophosphate was used as a single binder, this coincides with a low activity of the catalyst due to a major decrease in active sites, resulting in a low stability as well. In case of a binary binder system (combination of aluminophosphate and silica), the activity and lifetime of the catalyst was significantly improved, while the superior selectivity towards light olefins was not affected. Furthermore, the influence of transport through three dimensional catalysts has been evaluated. By altering the architecture of the catalyst, even better activity and lifetime of the catalyst was obtained with the same material composition. The activity and stability of the catalyst improved with decreasing fiber diameter. While with increasing porosity, the activity dropped but a large increase in stability was achieved. The selectivity on the other hand, was only slightly affected by changes in structural characteristics (fiber diameter and porosity). The silica/aluminophosphate ZSM-5 catalytic structure with 1-3 architecture (zigzag channels in the direction of the flow) exhibited an improved activity and stability compared to the 1-1 structure with straight channels due to tortuosity in the flow. The selectivity of the MTO reaction was mainly influenced by the active surface and acidity whereas the stability and activity were affected by composition as well as porosity, fiber thickness and stacking of the layers. This demonstrates that a simple change in binder or architecture of the catalyst has a major impact on its catalytic properties.

In future work, the combination of modeling with the experimental 3D-printing technique could allow even further tuning of the architecture in function of the application, catalysis, adsorption [36,37] or other. The possibilities are very broad, as the porosity, the wall thickness and the architecture of the channels can be altered independently of changes in catalyst properties and addition of promoting binders. Moreover, more complex designs are also possible: e.g. gradient structures with more or less catalyst at the wall or center, or at the top or bottom of the catalyst bed. Furthermore, the amount of binder and ratio of different binders can be altered according to the application. This work clearly shows that 3D-printing allows for rapid prototyping of composition and architecture of a catalyst and that catalysts with optimized composition can still be further improved by smart design.

Acknowledgement

J. Lefevere thankfully acknowledges a PhD scholarship provided by VITO and the University of Antwerp. This work was done in the frame of a project of the fund for scientific research (FWO) in Belgium (G. 007113N).

References

[1] T. Boger, A.K. Heibel, C.M. Sorensen, Monolithic Catalysts for the Chemical Industry, ChemInform. 35 (2004) 4602–4611. doi:10.1002/chin.200439250.

[2] C. Dai, Z. Lei, Q. Li, B. Chen, Pressure drop and mass transfer study in structured catalytic packings, Sep. Purif. Technol. 98 (2012) 78–87. doi:10.1016/j.seppur.2012.06.035.

[3] F.C. Patcas, G.I. Garrido, B. Kraushaar-Czarnetzki, CO oxidation over structured carriers: A comparison of ceramic foams, honeycombs and beads, Chem. Eng. Sci. 62 (2007) 3984–3990. doi:10.1016/j.ces.2007.04.039.

[4] G. Seijger, O. Oudshoorn, In situ synthesis of binderless ZSM-5 zeolitic coatings on ceramic foam supports, Microporous Mesoporous Mater. 39 (2000) 195–204. doi:10.1016/S1387-1811(00)00196-7.

[5] J. Zamaro, M. Ulla, E. Miro, Zeolite washcoating onto cordierite honeycomb reactors for environmental applications, Chem. Eng. J. 106 (2005) 25–33. doi:10.1016/j.cej.2004.11.003.

[6] Y. Liu, Z. Yang, C. Yu, X. Gu, N. Xu, Effect of seeding methods on growth of NaA zeolite membranes, Microporous Mesoporous Mater. 143 (2011) 348–356. doi:10.1016/j.micromeso.2011.03.016.

[7] Z. Shan, W.E.J. Van Kooten, O.L. Oudshoorn, J.C. Jansen, H. Van Bekkum, C.M. Van Den Bleek, H.P.A. Calis, Optimization of the preparation of binderless ZSM-5 coatings on stainless steel monoliths by in situ hydrothermal synthesis, Microporous Mesoporous Mater. 34 (2000) 81–91. doi:10.1016/S1387-1811(99)00161-4.

[8] A. Aranzabal, D. Iturbe, M. Romero-Sáez, M.P. González-Marcos, J.R. González-Velasco, J. a. González-Marcos, Optimization of process parameters on the extrusion of honeycomb

shaped monolith of H-ZSM-5 zeolite, Chem. Eng. J. 162 (2010) 415–423. doi:10.1016/j.cej.2010.05.043.

[9] A. Zamaniyan, Y. Mortazavi, A.A. Khodadadi, H. Manafi, Tube fitted bulk monolithic catalyst as novel structured reactor for gas–solid reactions, Appl. Catal. A Gen. 385 (2010) 214–223. doi:10.1016/j.apcata.2010.07.014.

[10] K. Shams, S.J. Mirmohammadi, Preparation of 5A zeolite monolith granular extrudates using kaolin: Investigation of the effect of binder on sieving/adsorption properties using a mixture of linear and branched paraffin hydrocarbons, Microporous Mesoporous Mater. 106 (2007) 268–277. doi:10.1016/j.micromeso.2007.03.007.

[11] Y.. Li, S.. Perera, B.. Crittenden, J. Bridgwater, The effect of the binder on the manufacture of a 5A zeolite monolith, Powder Technol. 116 (2001) 85–96. doi:10.1016/S0032-5910(00)00366-1.

[12] J.S.J. Hargreaves, A.L. Munnoch, A survey of the influence of binders in zeolite catalysis, Catal. Sci. Technol. 3 (2013) 1165. doi:10.1039/c3cy20866d.

[13] N.L. Michels, S. Mitchell, J. Pérez-Ramírez, Effects of binders on the performance of shaped hierarchical MFI zeolites in methanol-to-hydrocarbons, ACS Catal. 4 (2014) 2409–2417. doi:10.1021/cs500353b.

[14] K.-Y. Lee, H.-K. Lee, S.-K. Ihm, Influence of Catalyst Binders on the Acidity and Catalytic Performance of HZSM-5 Zeolites for Methanol-to-Propylene (MTP) Process: Single and Binary Binder System, Top. Catal. 53 (2009) 247–253. doi:10.1007/s11244-009-9412-0.

[15] L. V. MacDougall, Methanol to fuels routes. The achievements and remaining problems, Catal. Today. 8 (1991) 337–369. doi:10.1016/0920-5861(91)80057-G.

[16] Y. Zhuang, X. Gao, Y. Zhu, Z. Luo, CFD modeling of methanol to olefins process in a fixed-bed reactor, Powder Technol. 221 (2012) 419–430. doi:10.1016/j.powtec.2012.01.041.

[17] J. Lefevere, M. Gysen, S. Mullens, V. Meynen, J. Van Noyen, The benefit of design of support architectures for zeolite coated structured catalysts for alcohol-to-olefin conversion, Catal.

Today. 216 (2013) 18–23. doi:10.1016/j.cattod.2013.05.020.

[18] C.R. Tubío, J. Azuaje, L. Escalante, A. Coelho, F. Guitián, E. Sotelo, A. Gil, 3D printing of a heterogeneous copper-based catalyst, J. Catal. 334 (2016) 110–115. doi:10.1016/j.jcat.2015.11.019.

[19] X. Zhou, C. Liu, Three-dimensional Printing for Catalytic Applications : Current Status and Perspectives, 1701134 (2017) 1–13. doi:10.1002/adfm.201701134.

[20] Z. Wang, J. Wang, M. Li, K. Sun, C. Liu, Three-dimensional Printed Acrylonitrile Butadiene Styrene Framework Coated with Cu-BTC Metal-organic Frameworks for the Removal of Methylene Blue, Sci. Rep. 4 (2014) 4–10. doi:10.1038/srep05939.

[21] S. Danaci, L. Protasova, J. Lefevere, L. Bedel, R. Guilet, P. Marty, Efficient CO2 methanation over Ni/Al2O3 coated structured catalysts, Catal. Today. 273 (2016) 234–243. doi:10.1016/j.cattod.2016.04.019.

[22] S. Couck, J. Cousin Saint Remi, S. Van der Perre, G. V. Baron, C. Minas, P. Ruch, J.F.M. Denayer, 3D-printed SAPO-34 monoliths for gas separation, Microporous Mesoporous Mater. (2017). doi:10.1016/j.micromeso.2017.07.014.

[23] S. Couck, J. Lefevere, S. Mullens, L. Protasova, V. Meynen, G. Desmet, G. V. Baron, J.F.M. Denayer, CO2, CH4 and N2 separation with a 3DFD-printed ZSM-5 monolith, Chem. Eng. J. 308 (2017) 719–726. doi:10.1016/j.cej.2016.09.046.

[24] H. Thakkar, S. Eastman, A. Hajari, A.A. Rownaghi, J.C. Knox, F. Rezaei, 3D-Printed Zeolite Monoliths for CO2 Removal from Enclosed Environments, ACS Appl. Mater. Interfaces. 8 (2016) 27753–27761. doi:10.1021/acsami.6b09647.

[25] J. Luyten, S. Mullens, I. Thijs, Designing With Pores–Synthesis and Applications, KONA Powd. Part. J. 28 (2010) 131–142. http://121.83.250.58/search/28_131.pdf (accessed October 11, 2012).

[26] W. Guo, W. Wu, M. Luo, W. Xiao, Modeling of diffusion and reaction in monolithic catalysts for the methanol-to-propylene process, Fuel Process. Technol. (2012) 6–11.

doi:10.1016/j.fuproc.2012.06.005.

[27] W. Guo, W. Xiao, M. Luo, Comparison among monolithic and randomly packed reactors for the methanol-to-propylene process, Chem. Eng. J. 207–208 (2012) 734–745. doi:10.1016/j.cej.2012.07.046.

[28] M. Rombouts, S. Mullens, J. Luyten, P. Nuyts, M. Schroeven, The production of Ti-6Al-4V parts with controlled porous architecture by three-dimensional fiber deposition, in: et al. P. J., da Silva Bartolo (Ed.), Innov. Dev. Des. Manuf., CRC Press, 2010: pp. 453–457.

[29] J. Lefevere, L. Protasova, S. Mullens, V. Meynen, 3D-printing of hierarchical porous ZSM-5: The importance of the binder system, Mater. Des. 134 (2017) 331–341. doi:10.1016/j.matdes.2017.08.044.

[30] C.J. Van Oers, K. Go, J. Datka, V. Meynen, P. Cool, Demonstrating the Benefits and Pitfalls of Various Acidity Characterization Techniques by a Case Study on Bimodal Aluminosilicates, Langmuir. 30 (2014) 1880–1887.

[31] Y.-J. Lee, Y.-W. Kim, N. Viswanadham, K.-W. Jun, J.W. Bae, Novel aluminophosphate (AlPO) bound ZSM-5 extrudates with improved catalytic properties for methanol to propylene (MTP) reaction, Appl. Catal. A Gen. 374 (2010) 18–25. doi:10.1016/j.apcata.2009.11.019.

[32] J. Freiding, F.-C. Patcas, B. Kraushaar-Czarnetzki, Extrusion of zeolites: Properties of catalysts with a novel aluminium phosphate sintermatrix, Appl. Catal. A Gen. 328 (2007) 210–218. doi:10.1016/j.apcata.2007.06.017.

[33] G.T. Whiting, F. Meirer, M.M. Mertens, A.J. Bons, B.M. Weiss, P.A. Stevens, E. De Smit, B.M. Weckhuysen, Binder effects in SiO<inf>2</inf>- and Al<inf>2</inf>O<inf>3</inf>-bound zeolite ZSM-5-based extrudates as studied by microspectroscopy, ChemCatChem. 7 (2015) 1312–1321. doi:10.1002/cctc.201402897.

[34] G.T. Whiting, A.D. Chowdhury, R. Oord, P. Paalanen, B.M. Weckhuysen, The curious case of zeolite–clay/binder interactions and their consequences for catalyst preparation, Faraday Discuss. 188 (2016) 369–386. doi:10.1039/C5FD00200A.

[35] M. Bjorgen, S. Svelle, F. Joensen, J. Nerlov, S. Kolboe, F. Bonino, L. Palumbo, S. Bordiga, U. Olsbye, Conversion of methanol to hydrocarbons over zeolite H-ZSM-5: On the origin of the olefinic species, J. Catal. 249 (2007) 195–207. doi:10.1016/j.jcat.2007.04.006.

[36] S. Couck, J. Lefevere, S. Mullens, L. Protasova, V. Meynen, G. Desmet, G. V Baron, J.F.M. Denayer, CO2, CH4 and N2 separation with a 3DFD-printed ZSM-5 monolith, Chem. Eng. J. 308 (2017) 719–726. doi:10.1016/j.cej.2016.09.046.

[37] H. Thakkar, S. Eastman, Q. Al-Naddaf, A.A. Rownaghi, F. Rezaei, 3D-Printed Metal–Organic Framework Monoliths for Gas Adsorption Processes, ACS Appl. Mater. Interfaces. (2017) acsami.7b11626. doi:10.1021/acsami.7b11626.

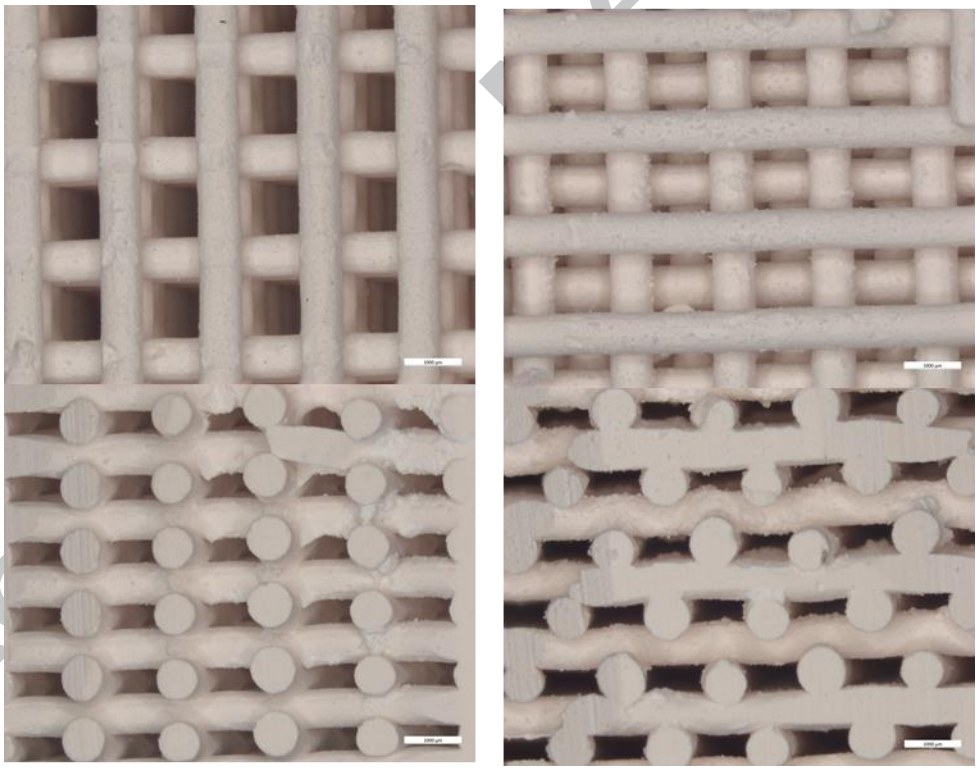

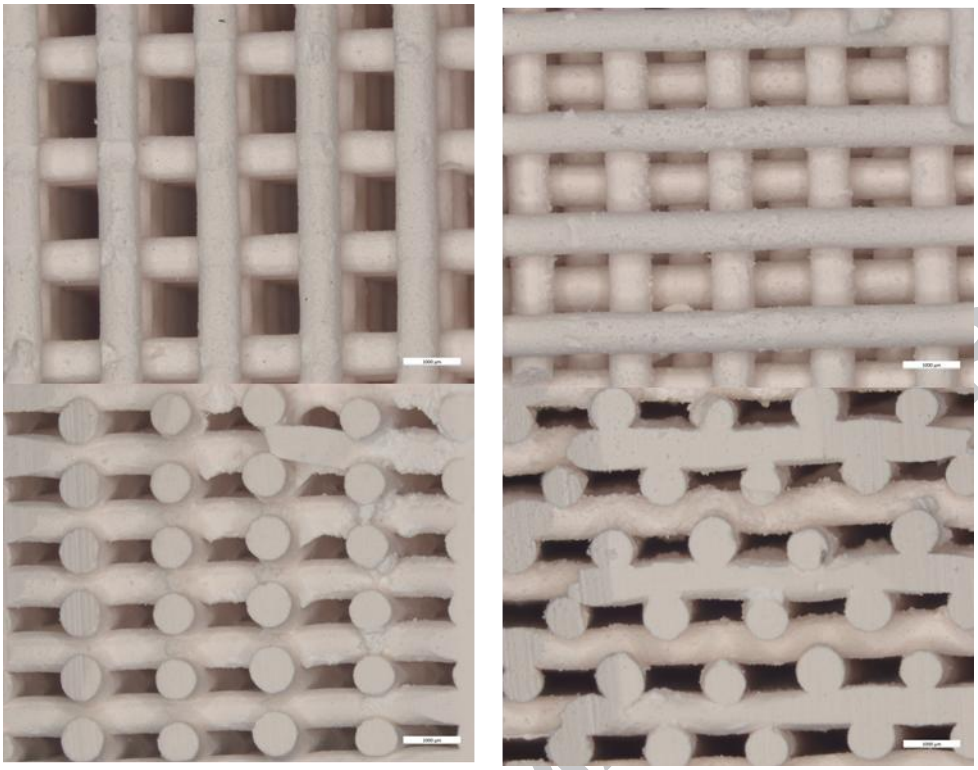

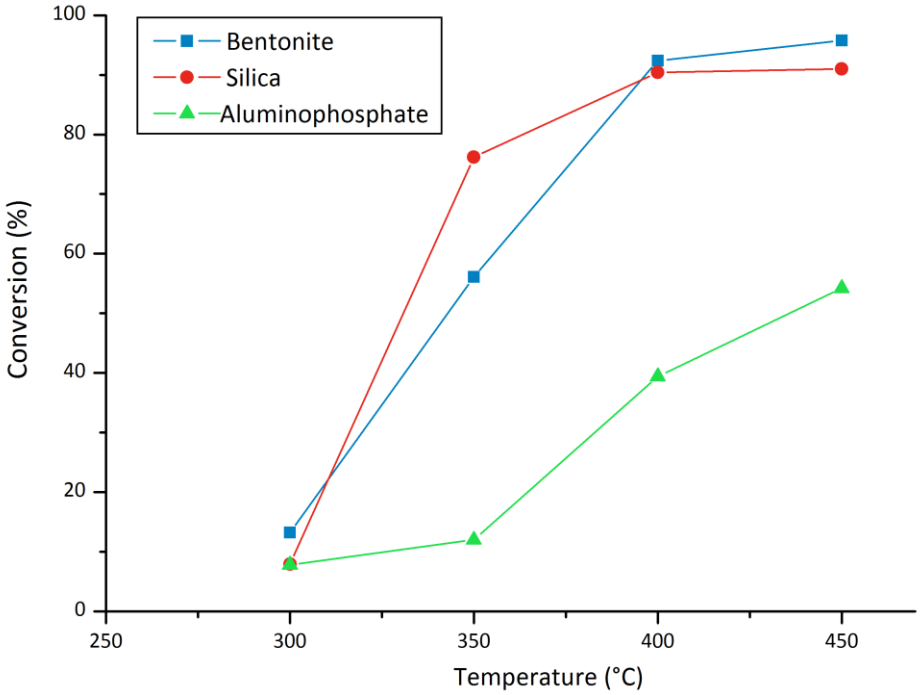

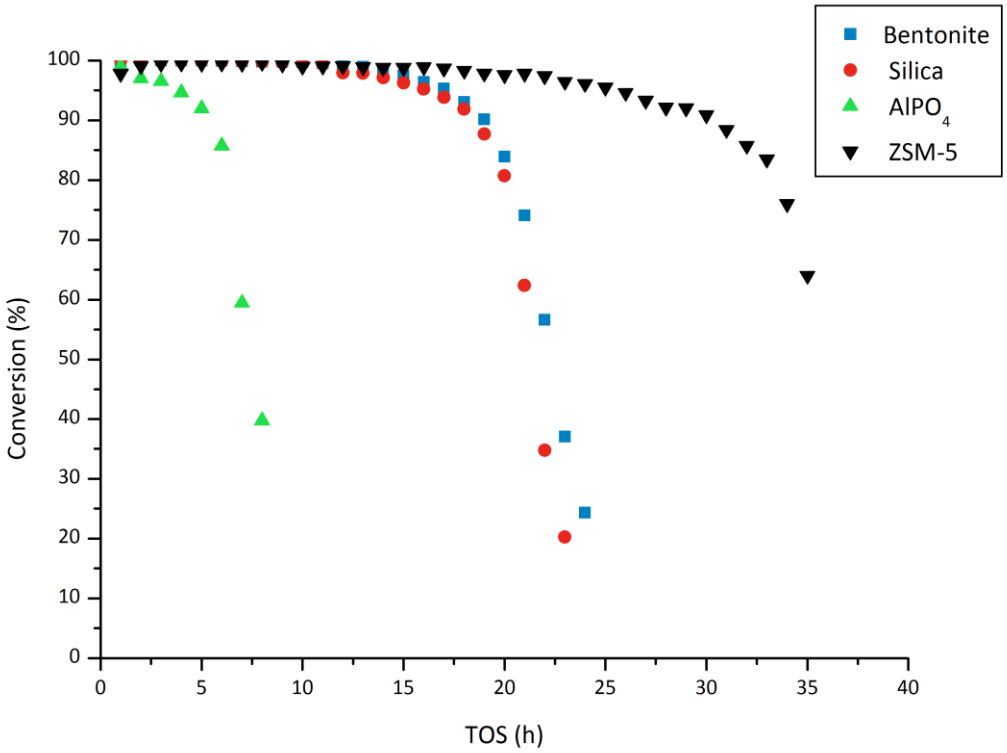

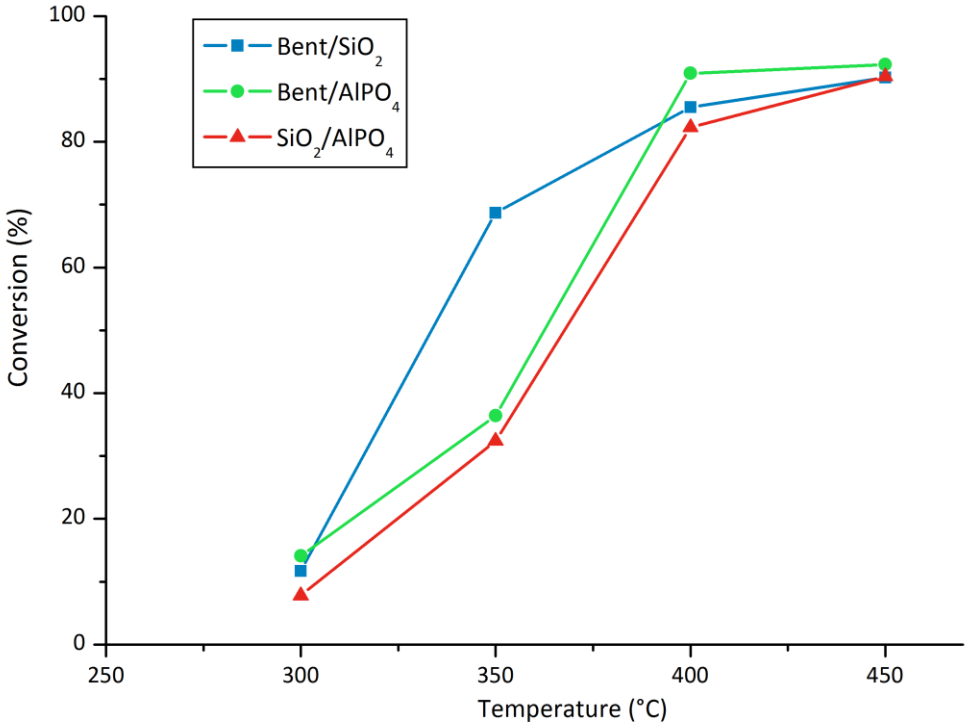

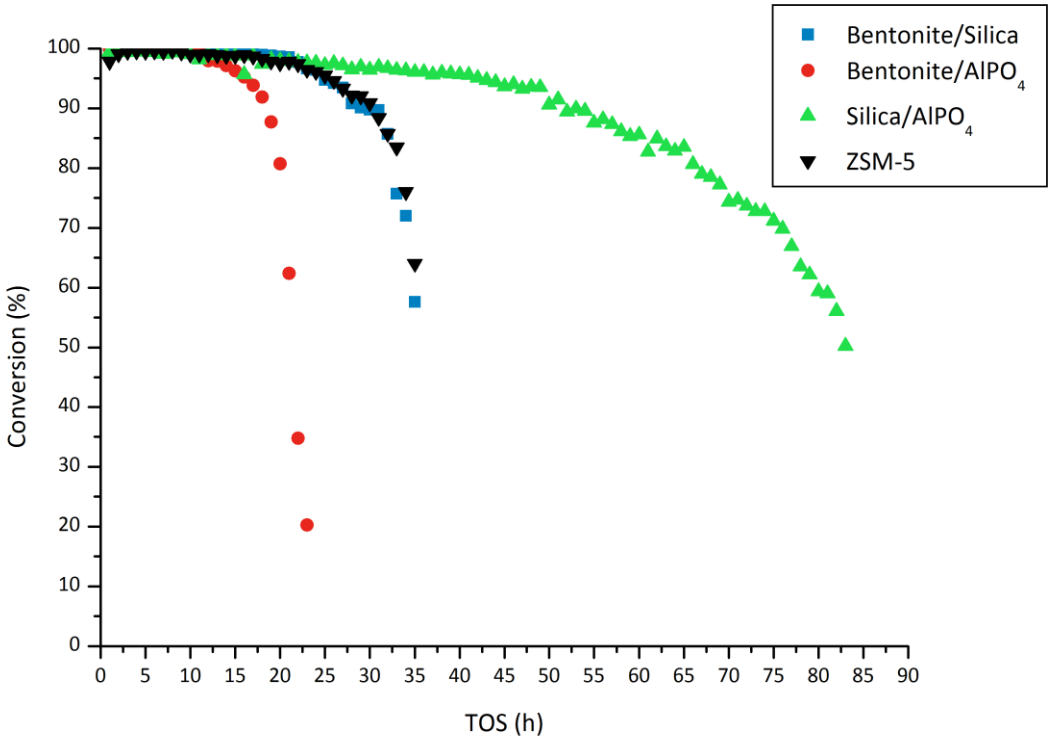

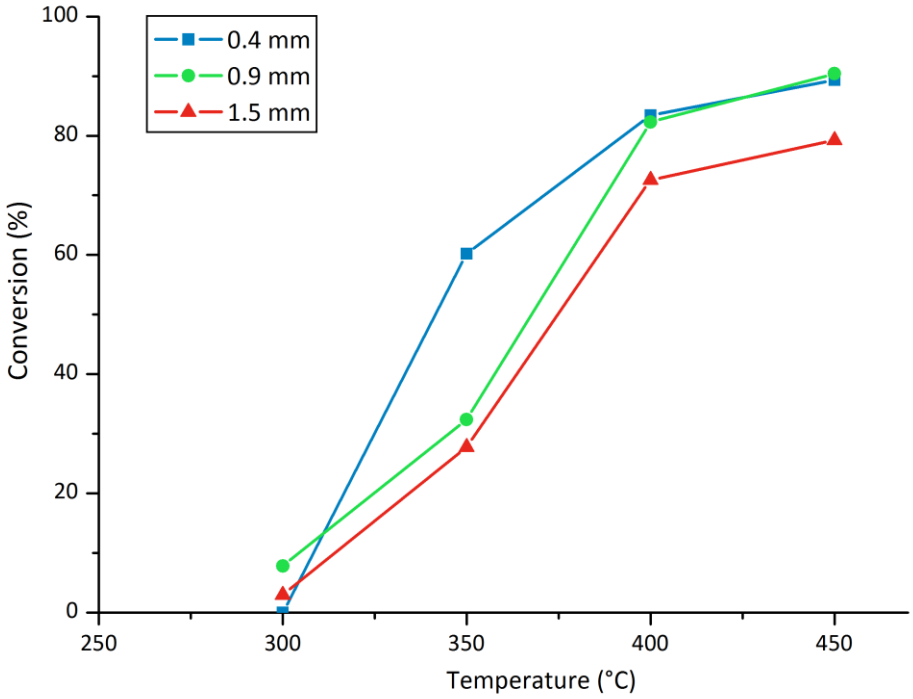

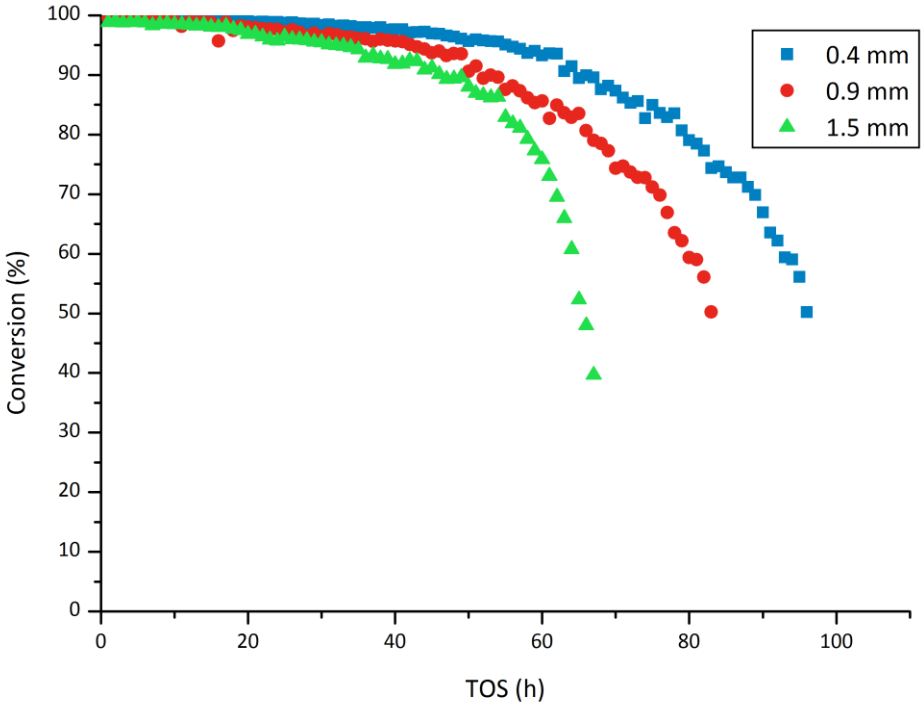

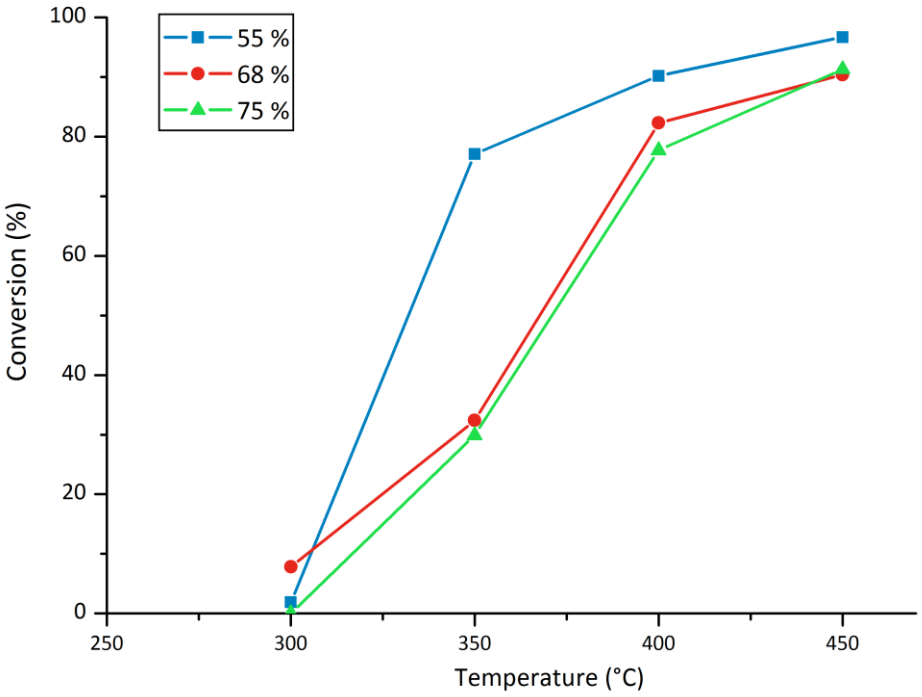

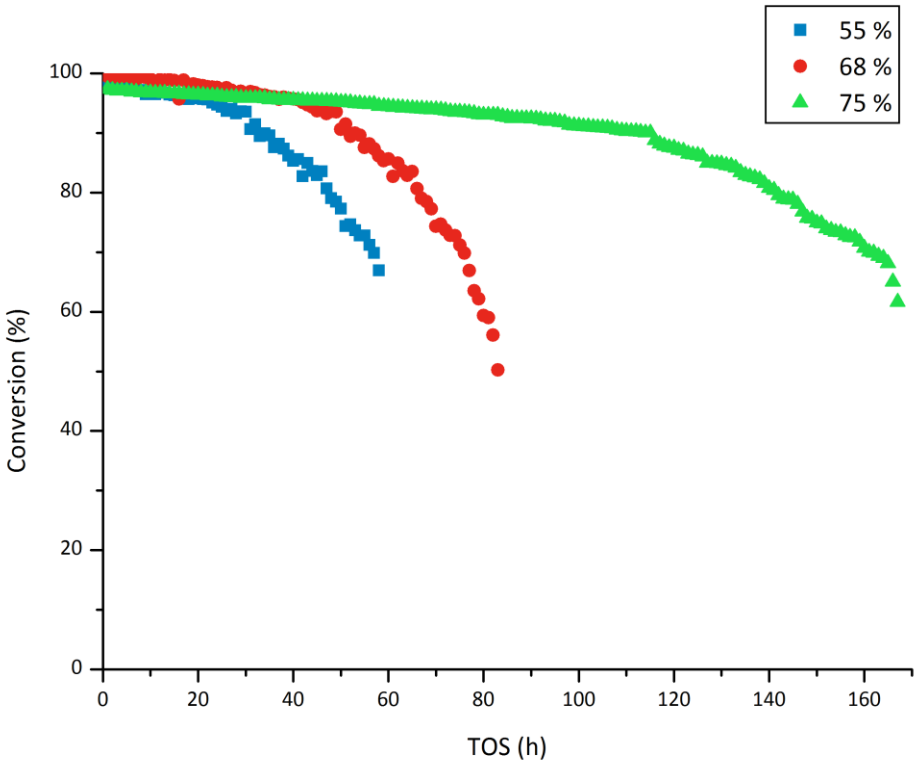

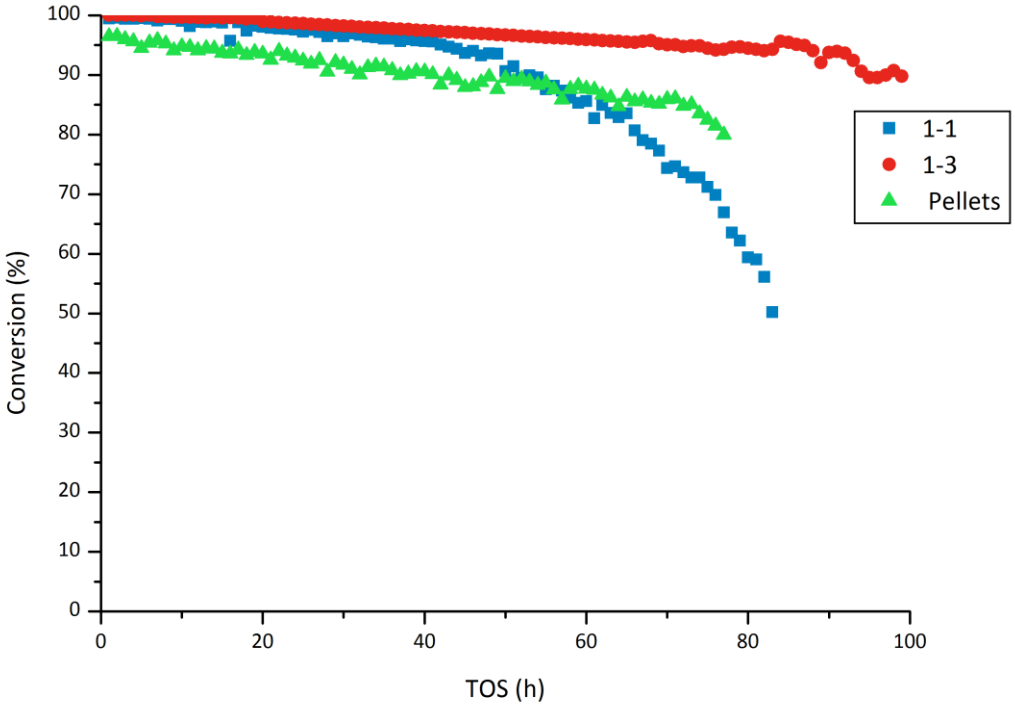

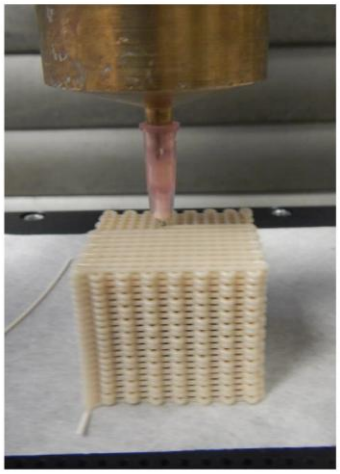

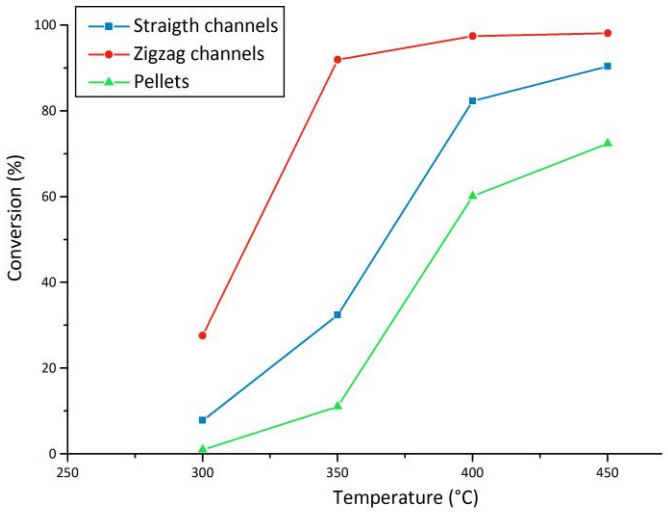

- 3D-printed ZSM-5 monoliths with different binders and 3D-design were compared in MTO.
- The combination of SiO_2/$AlPO_4$ as binders resulted in improved catalytic properties.
- Smaller fiber diameter and higher porosity resulted in higher stability.
- Enhanced catalytic performance was reached with altered stacking of the layers
- This technique allows for optimization of composition and 3D design of catalysts.